

Radiation-enhanced impurity aggregation in MgO

S. Clement and E. R. Hodgson

División de Fusión, Junta de Energía Nuclear, 28040 Madrid, Spain

(Received 22 December 1986)

Electron irradiation at high temperatures of pure, Fe-, and Ni-doped MgO suppresses the Fe^{3+} and Ni^{2+} optical absorption bands, and leads to the production of precipitates containing Fe and Ni. The results suggest metallic precipitates. This process is due to radiation-induced reduction and precipitation, in which displacement damage and radiation-enhanced diffusion play an important role. In the case of Fe, the results indicate Fe^{2+} as the diffusing entity. Comparison between electron and γ -ray irradiations show that Fe^{2+} ions which are paired with other impurities do not readily diffuse under electron irradiation.

I. INTRODUCTION

Over the years considerable work has been carried out on thermally stimulated impurity diffusion and aggregation in MgO.¹⁻⁴ However, to date, little if any information exists as to the influence of radiation on the impurity diffusion, only that of hydrogen being documented.⁵

It is well known that the presence of transition-metal impurities in refractory oxides affects quite markedly the optical, electrical, and mechanical properties. The effect is strongly dependent on the valence and aggregation state of the impurity, and in particular the case of iron in MgO is well documented.^{1,6-9} At low concentrations iron is present in a substitutional form as Fe^{2+} and Fe^{3+} , and may be changed from one valence state to another by purely ionizing radiation at room temperature, due to electron capture at other impurities,^{6,10-12} or by reduction or oxidation at high temperatures ($\geq 1100^\circ\text{C}$).¹³ While Fe^{3+} has an adverse effect on the uv optical transmission and electrical breakdown properties,^{6,9} its presence, even in small concentrations, notably increases the hardness of MgO, and appears at higher concentrations to play a role in the formation of spinel regions within the lattice.¹⁴

In view of the importance of impurities such as iron, and bearing in mind the technological application of refractory oxides in any future fusion reactor, it is clearly of importance to study the behavior of such impurities under the expected severe conditions of radiation and temperature. To do this, measurements have been made, electron irradiating MgO at high dose rates and temperatures. The results show a suppression of the Fe^{3+} above about 600°C which is dependent on both dose rate and temperature. Radiation-enhanced diffusion gives rise to precipitates containing iron at much lower temperatures than observed in thermochemical reduction. The observed extent of the effect strongly suggests that oxygen displacement damage is involved in the reduction of the Fe^{3+} , and comparison between γ -ray and electron irradiations points to Fe^{2+} as the diffusing entity. Similar results have been obtained in nickel-doped MgO, confirming the importance of radiation-enhanced impurity diffusion and precipitation at relatively low temperatures.

II. EXPERIMENTAL PROCEDURE

The experimental chamber is mounted in the beam line of a 2-MeV HVEC Van de Graaff accelerator, and permits sample irradiation in high vacuum ($\sim 2 \times 10^{-6}$ torr) either directly with up to 2-MeV electrons or with bremsstrahlung γ -rays produced by stopping the electron beam in a gold target.

The samples ($\sim 5 \times 5 \times 1$ mm³) are sandwiched between a double oven and irradiated edge on, on one of the (5×1) -mm² faces. Two (3×1) -mm² windows cut in the ovens enable *in situ* measurements of optical absorption to be made perpendicular to the irradiation direction at a distance of 1–2 mm behind the irradiated face. The samples may be linearly heated from 10 to 950°C and maintained at any intermediate temperature to within 1°C . During direct electron irradiation the beam current may be maintained to within 5% of the nominal value, giving a sample temperature variation of about $\pm 10^\circ\text{C}$.

In this way three types of MgO single-crystal samples have been studied: nominally pure samples containing between 160 and 180 ppm Fe (99.99% pure from W.C. Spicer) and Fe- and Ni-doped samples containing approximately 1500 and 3000 ppm Fe and Ni, respectively (by courtesy of Dr. Y. Chen, Oak Ridge¹⁵). The pure samples have been electron irradiated at 1.8 MeV, $60 \mu\text{A cm}^{-2}$, for sample temperatures of 360, 550, 650, and 750°C , and at $120 \mu\text{A cm}^{-2}$, 650, and 750°C . The Fe- and Ni-doped samples were electron irradiated at $120 \mu\text{A cm}^{-2}$, 650°C , and $90 \mu\text{A cm}^{-2}$, 750°C . In addition, one pure sample was alternately irradiated with bremsstrahlung γ -rays at 14°C , 3.5×10^4 rad h⁻¹, and 1.8 MeV electrons at $60 \mu\text{A cm}^{-2}$, 800°C . The γ irradiations were all of 8 h duration and served as a way of monitoring the amount of Fe^{2+} converted to Fe^{3+} by electron capture at other impurities, and the effect of the high-temperature electron irradiations on this process. For all the experiments an initial spectrum was taken at 14°C following heating of the sample to the irradiation temperature, and thereafter at varying time intervals during the irradiations, again at 14°C .

The pure and doped samples irradiated at 650°C , $120 \mu\text{A cm}^{-2}$ were thinned by the jet polishing technique with phosphoric acid and observed in a transmission electron microscope. X-ray fluorescence spectra were obtained for the precipitates observed.

III. RESULTS

Figures 1(a), 1(b), and 1(c) show the initial and final spectra for the pure, Fe- and Ni-doped samples irradiated at 650°C $120 \mu\text{A cm}^{-2}$. One observes an almost complete suppression of the Fe^{3+} band at 290 nm [(a) and (b)], and in the case of the Ni-doped sample (c), a partial suppression of the Ni^{2+} bands at 400 and 670 nm, together with the growth of a broadband at around 400 nm. Following the initial suppression, the pure and Fe-doped samples showed very little change after 8 and 24 h of irradiation, respectively, whereas for the Ni-doped sample the absorption continued to increase notably after 23 h of irradiation. Very similar results have been obtained for the pure samples irradiated at 750°C , 60 and $120 \mu\text{A cm}^{-2}$, and 800°C , $60 \mu\text{A cm}^{-2}$, and the Fe- and Ni-doped samples at 750°C , $90 \mu\text{A cm}^{-2}$. In Fig. 2

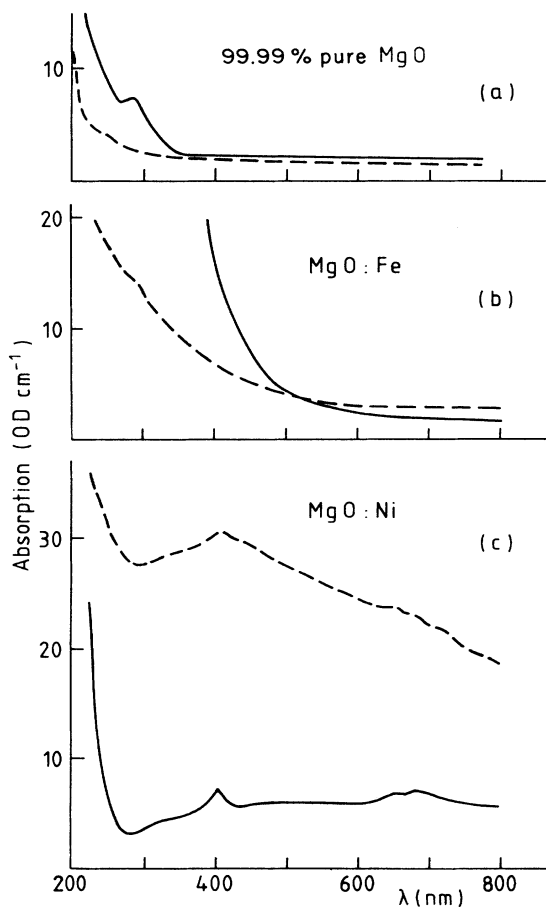


FIG. 1. Initial (solid lines) and final (dashed lines) spectra for (a) pure MgO, (b) MgO:Fe, and (c) MgO:Ni all irradiated at 650°C $120 \mu\text{A cm}^{-2}$ for 19, 41, and 23 h, respectively. The absorption for this and Figs. 2, 3, and 5, is given in optical density cm^{-1} , (OD cm^{-1}).

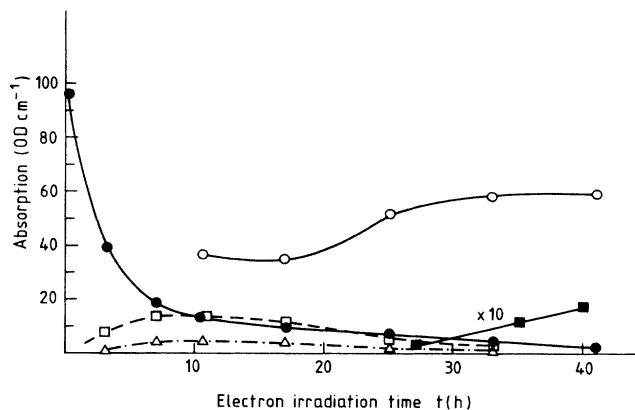


FIG. 2. Optical-absorption-band results for MgO:Fe irradiated at 650°C $120 \mu\text{A cm}^{-2}$, showing the evolution of bands at 290 nm (Fe^{3+} , closed circles), 280 nm (triangles), 240–250 nm (open squares), uv below 210 nm (open circles), and the general background (closed squares).

the absorption spectra results for the Fe-doped sample irradiated at 650°C , $120 \mu\text{A cm}^{-2}$, for 41 h are shown. As the Fe^{3+} band decreases, bands at about 250 and 280 nm are observed to grow and then decrease as the far-uv region and then the general background increase. The 250-nm band was complex and consisted of two bands at about 240 and 250 nm. Figure 3 shows the absorption band variations for the Ni-doped sample irradiated at 750°C , $90 \mu\text{A cm}^{-2}$, for 23 h. While the two Ni^{2+} bands decrease linearly with irradiation time, a very broad band at about 400 nm grows rapidly. In Fig. 4 the Fe^{3+} band suppression observed in the pure samples for different dose rates and temperatures is shown as a function of irradiation time. The suppression is observed above about 550°C and is strongly enhanced by increasing dose rate and/or temperature. The initial rapid increase observed at 360, 550, and 650°C is due to purely electronic processes in which $\text{Fe}^{2+} \rightarrow \text{Fe}^{3+}$.

Figure 5 shows the results obtained for the alternate γ and electron irradiations, where the amount of γ -ray-induced Fe^{3+} is given as a function of electron irradiation time. One observes an increase in the first six hours of electron irradiation, and then little change up to 38 h. An Arrhenius plot of the time to suppress the Fe^{3+} band to half of its initial value is given in Fig. 6 for the nominally pure samples irradiated at $60 \mu\text{A cm}^{-2}$ and temperatures between 550 and 800°C . The slope gives an activation energy of $1.5 \pm 0.3 \text{ eV}$ for the associated process. Values at double the dose rate ($120 \mu\text{A cm}^{-2}$) for 650 and 750°C are also shown for comparison.

Following irradiation both the Fe- and Ni-doped samples undergo notable color changes. The Fe-doped samples lose their characteristic yellow color to a depth of about 3 mm in the irradiation direction and turn a grayish color. The green Ni-doped samples turn black, again to a depth of about 3 mm. Small pieces of these regions are magnetic for both the Fe- and Ni-doped samples. The electron microscope results show the presence of

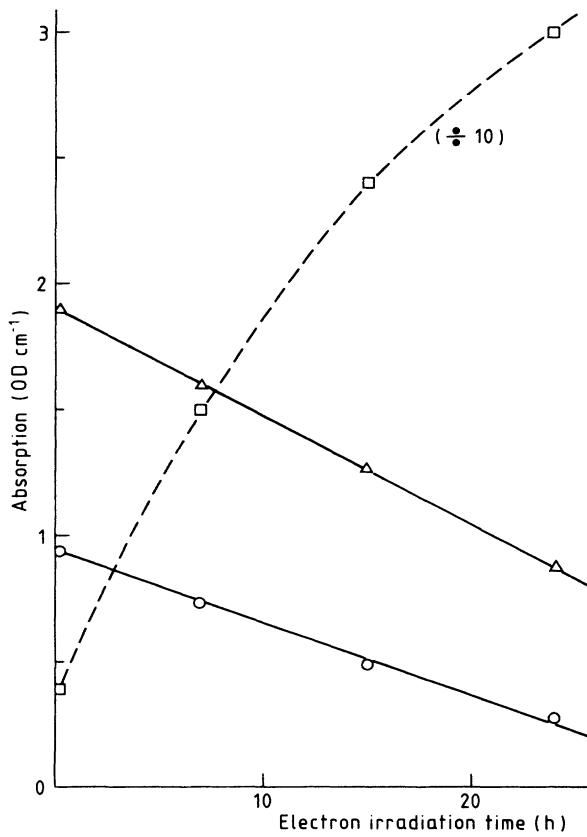


FIG. 3. Optical-absorption-band results for MgO:Ni irradiated at 750°C 90 $\mu\text{A cm}^{-2}$, showing the evolution of the Ni^{2+} bands at 400 nm (triangles) and 670 nm (circles), together with the broadband at about 400 nm (squares).

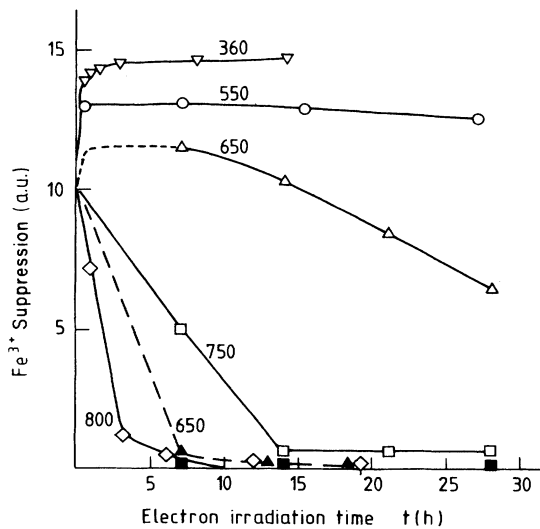


FIG. 4. Fe^{3+} suppression for pure MgO irradiated at 60 $\mu\text{A cm}^{-2}$ (open symbols) and 120 $\mu\text{A cm}^{-2}$ (closed symbols) for temperatures between 360 and 800°C. The 120 $\mu\text{A cm}^{-2}$ 750°C case (closed squares) coincides closely with the 60 $\mu\text{A cm}^{-2}$ 800°C case and is not shown for clarity. The initial values are normalized to 10.

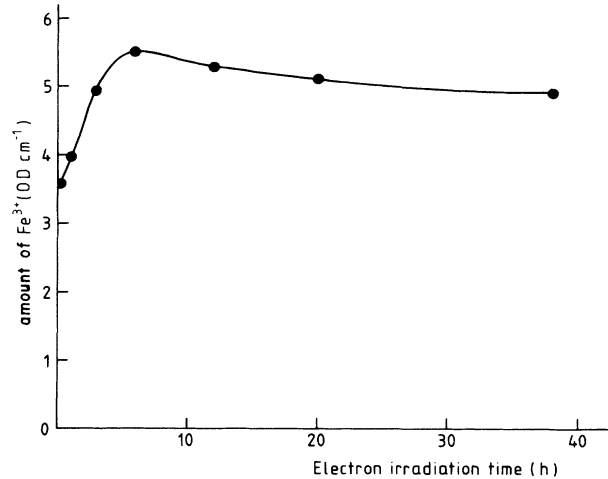


FIG. 5. The amount of Fe^{3+} induced by a standard 8 h 14°C γ irradiation, as a function of 60 $\mu\text{A cm}^{-2}$ 800°C electron irradiation time.

precipitates in the pure, Fe-, and Ni-doped samples, at a much higher density in the doped samples, both uniformly distributed and decorating dislocation lines. Figure 7 shows three typical electron micrographs for the pure and iron-doped samples. Qualitative energy-dispersive x-ray fluorescence spectra show that the pre-

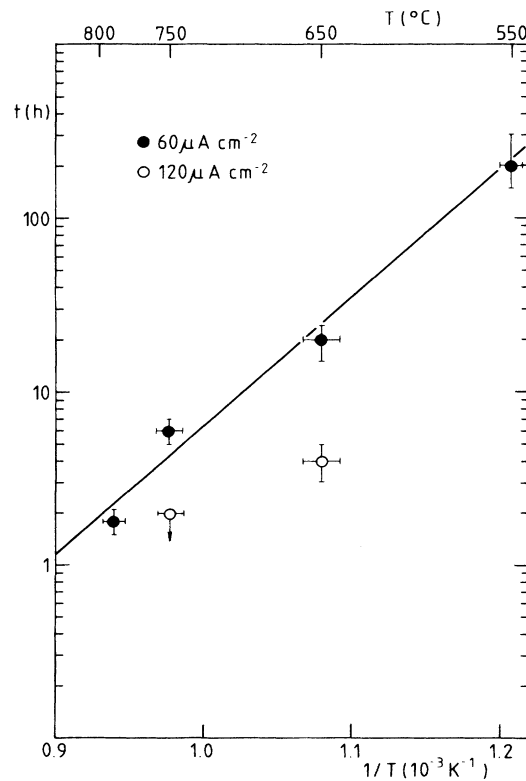


FIG. 6. Log plot of the time to suppress the Fe^{3+} band to half its initial value as a function of $1/T$, for the nominally pure samples irradiated at 60 $\mu\text{A cm}^{-2}$. The two 120 $\mu\text{A cm}^{-2}$ cases are also shown for comparison.

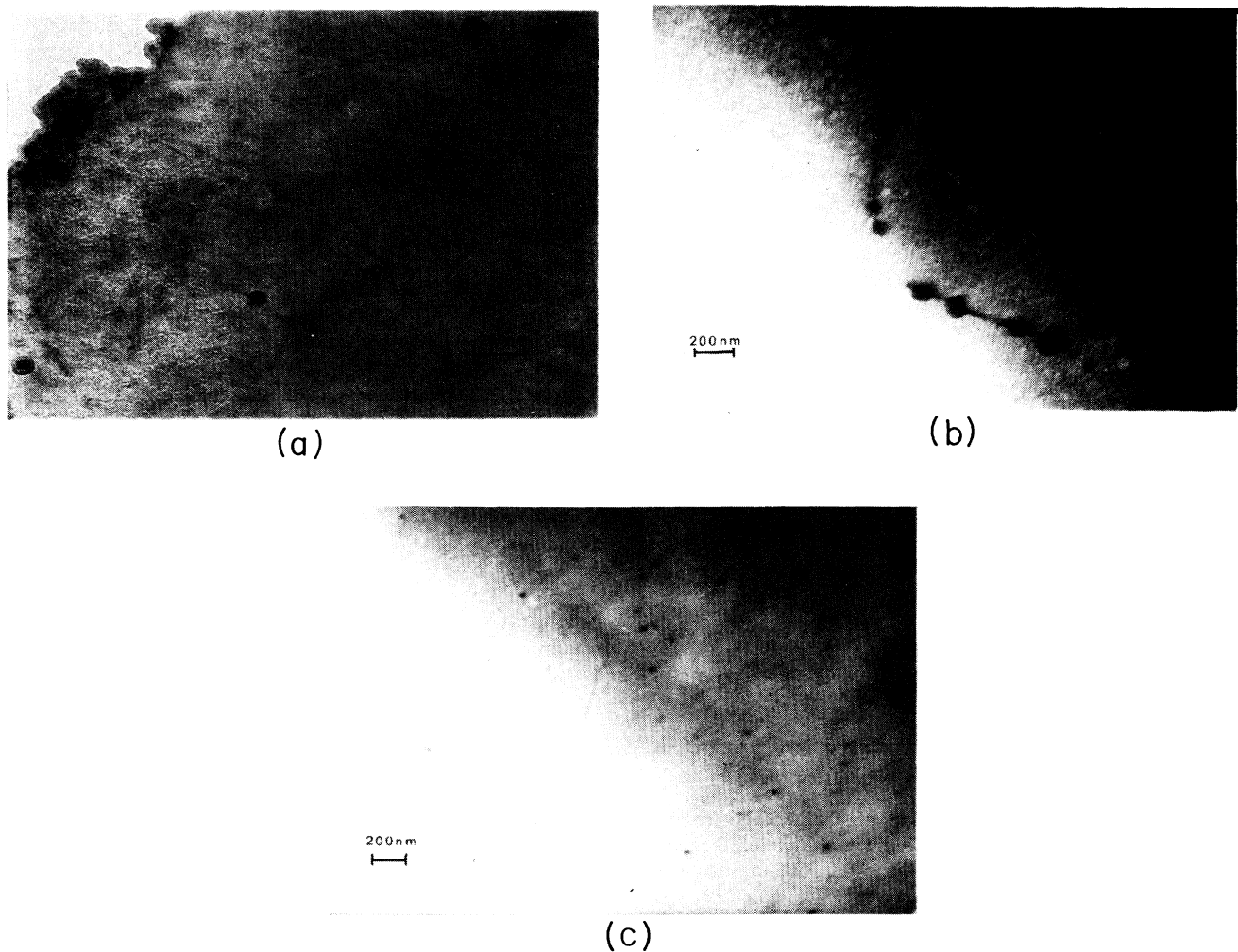


FIG. 7. Electron micrographs showing iron-containing precipitates in the pure (a) and iron-doped samples (b) and (c) following irradiation at 650°C, 120 $\mu\text{A cm}^{-2}$.

precipitates contain iron in the pure and Fe-doped samples, and nickel in the Ni-doped samples. The precipitates in the pure sample have been observed following only 19 h of irradiation. Calculations from the precipitate size and number indicate that they contain over about 30% of the iron or nickel present in the irradiated part of the samples. No precipitates have been observed beyond about 3 mm behind the irradiated face. Furthermore, in this region for the pure samples, an increase is observed in the Fe^{3+} band, contrasting with the complete suppression observed at between 1 and 2 mm behind the irradiated face.

IV. DISCUSSION

To date, data available for MgO in general indicate an increase of the Fe^{3+} band with irradiation time, which may be annealed on heating to below about 650°C. These effects are attributed to charge-transfer processes involving Fe^{2+} and other impurities, induced by the ionizing radiation.^{6,10-12} Little information if any exists as to the effect on the impurities of high-dose-rate particle

irradiation at high temperatures. The results presented here indicate that under these conditions Fe^{3+} is suppressed [Figs. 1(a) and 1(b)]. As may be seen in Fig. 4, this effect becomes important at temperatures above about 550°C and is a strong function of dose rate. The end result of the radiation-induced suppression process is the production of iron-containing precipitates. The fact that small pieces of the doped samples were found to be magnetic suggests metallic precipitates.^{1,4} The Ni-doped samples [Figs. 1(c) and 3] also show a suppression, in the Ni^{2+} bands in this case, together with a strong increase in the background and Ni-containing precipitates are formed.

Decreases in the Fe^{3+} content,¹⁶ or evidence for suppression processes,¹⁷ have been observed under purely ionizing radiation due to hole transfer giving rise to Fe^{2+} , but in contrast with the results presented here, these effects are unstable by 100°C. There are no reported cases of Fe^{4+} in MgO, either before or after irradiation. High-temperature Fe^{3+} and Ni^{2+} suppression and precipitation have been observed in thermochemical reduction experiments at above about 1000°C, well in excess of the

temperatures reported here.^{1,2,4,13,18-21} However, the general results are remarkably similar to those observed here (absorption bands, color changes, precipitates).

The doped samples permitted a more detailed study of the process. Figure 2 shows the absorption spectra results for the MgO: Fe, in which not only the Fe³⁺ suppression is observed, but also the growth of bands at about 250 and 280 nm, together with an increase in the far-uv region and general background. Calculations based on Doyle's theory indicate a band at about 160 nm for small metallic Fe colloids in MgO³. This is consistent with the observed increase in the far-uv region, and the fact that the samples were found to be magnetic. The general background increase would then be due to scattering from larger precipitates (precipitates up to ~50 nm in size have been found). The fact that this increase occurs at a later stage is consistent with precipitate growth.²²

An intermediate stage is observed in which bands at about 250 and 280 nm grow as the Fe³⁺ decreases and then decrease as the precipitates begin to form. A residual band at about 280 nm has been previously observed in reduced MgO and tentatively suggested to be due to Fe³⁺ associated with aggregates or vacancies.¹³ Apart from the well-known *F*-center bands at about 250 nm, a band at 253 nm has been observed in highly reduced MgO and attributed to Fe²⁺.¹⁸

The MgO:Ni absorption spectra results (Fig. 3) show that, as the Ni²⁺ bands decrease, a broadband at about 400 nm grows strongly. An exactly identical effect has been observed in reduced MgO:Ni and attributed to the growth of small Ni colloids.²¹

All these observations strongly suggest that we are dealing with a radiation-induced reduction and precipitation process. In thermochemical reduction, even the first-stage Fe³⁺ → Fe²⁺ has only been observed at temperatures ≥ 900 °C (at 960 °C this first stage is about 25 times slower than our 650 °C case¹⁹). We must therefore be dealing with a radiation-enhanced process.

It is believed that thermochemical impurity reduction in MgO involves oxygen-ion vacancies.^{20,21} These vacancies are created by chemical reaction at the surface and diffuse into the bulk. In our case, apart from the initial intrinsic anion vacancies, far too few to account for the amount of Fe and Ni reduced, vacancies are produced in the bulk by direct knock-on displacement damage. To date there is little or no evidence for a radiolysis process similar to that observed in the alkali halides. The Fe and Ni reduction and precipitation has only been observed in the samples to a depth corresponding to the 1.8-MeV electron range in MgO (~3 mm), strongly suggesting that displacement damage is indeed necessary. The fact that beyond this range where there is only purely ionizing radiation the entirely opposite effect occurs (the Fe³⁺ increases), supports this view. We cannot be dealing with a direct interaction of the electron beam with the Fe and Ni ions, because in this case the necessary cross section would be ~10⁵ b, typical of purely ionizing processes, and this is not observed. However, assuming that the necessary vacancies for reduction are produced by oxygen-displacement damage, the lower limit for the oxygen-displacement cross section

based on the reduction rate of the Fe³⁺ and Ni²⁺ is 5 b. This value is in good agreement with theoretical calculations for oxygen displacement in MgO.²³ The value is higher than that found in *F*-center production experiments,^{24,25} but in our temperature and dose-rate range large dislocation loops have been observed to grow, implying the formation of very effective interstitial traps.²⁶

Apart from the initial fast increase observed in the Fe³⁺ band at the lower temperatures (Fig. 4), due to the charge-transfer processes involving Fe²⁺ and which are unstable above 650 °C,^{11,12} the data indicate an Fe³⁺ and Ni²⁺ suppression with irradiation time which is a function of temperature and dose rate. The activation energy associated with the Fe³⁺ reduction, obtained from the data for the pure samples (Fig. 6), is 1.5 ± 0.3 eV. This is considerably lower than values found in thermochemical reduction experiments [between ~2.2 and 3.2 eV (Refs. 27 and 28)]. This low value is consistent with the vacancy diffusion being enhanced by the ionizing dose rate. Such a reduction in activation energy has been observed for the *F* center in NaCl under radiation.²⁹ The radiation enhancement is supported by the fact that doubling the dose rate more than doubles the Fe³⁺ reduction rate (Fig. 6). Doubling the dose rate (beam current) not only doubles the vacancy production rate but also doubles the ionizing dose rate. Hence, if we are dealing with radiation-enhanced vacancy diffusion, the Fe³⁺ reduction rate should vary as the square of the dose rate increases. Table I gives the expected effect of increasing the beam current by a factor 1.5 and 2, together with the observed effect on the Fe³⁺ reduction time. As may be seen, to within the experimental errors, the effect of increasing the dose rate is consistent with a radiation-enhanced vacancy diffusion process.

To form Fe (and Ni) precipitates, the impurity must diffuse in some form within the lattice. As discussed above, the Fe³⁺ suppression is due to a radiation-induced reduction process, presumably giving rise to Fe²⁺ which then either diffuses directly as Fe²⁺, or is further reduced before diffusion. The alternate γ and electron irradiations help to throw light on this question. Figure 5 shows the amount of Fe³⁺ induced by an 8-h γ irradiation at 14 °C as a function of electron irradiation time at 800 °C. As may be seen in Fig. 3, the electron irradiation almost completely suppresses the Fe³⁺ in about 3 h, whereas the γ -ray-induced Fe³⁺ even shows an increase in the first 6 h of electron irradiation. Clearly two different types of Fe³⁺ are involved: the Fe³⁺ stable at 800 °C but suppressed under electron irradiation, and the Fe³⁺ un-

TABLE I. The expected effect of increasing the beam current from 60 to 90 and 60 to 120 $\mu\text{A cm}^{-2}$, compared with the observed effect on the Fe³⁺ suppression rate at 650 and 750 °C.

	Fe ³⁺ suppression rate	
	60 → 90 $\mu\text{A cm}^{-2}$	60 → 120 $\mu\text{A cm}^{-2}$
Expected	2.25 ± 0.2	4.0 ± 0.3
650 °C		5.0 ± 1.7
750 °C	2.4 ± 0.4	3.0 ^{+2.0} _{-0.5}

stable by 650°C, induced by the γ irradiation due to charge-transfer processes involving Fe^{2+} and other impurities.^{6,10-12} In some way these Fe^{2+} ions do not diffuse and precipitate; even after 38 h of electron irradiation their number shows very little decrease after the initial maximum at 6 h (Fig. 5). Under these electron irradiation conditions, iron precipitates containing over 30 at. % of the total iron content are observed in less than 20 h. This would only be reasonable if the Fe^{2+} ions involved in the charge-transfer processes were associated with the other impurity in some way which inhibits their diffusion. This is in agreement with earlier results which suggest that they are in close proximity within the lattice.^{12,17} If during electron irradiation unassociated Fe^{2+} ions and Fe^{2+} ions produced by the radiation-induced reduction of isolated Fe^{3+} ions diffuse, they could associate with other impurities as well as precipitate. This process would be clearly limited by the availability of other suitable impurities, and would explain the saturating growth of the γ -ray-induced Fe^{3+} (Fig. 5). These observations are consistent with the fact that the amount of γ -ray-induced Fe^{3+} is not a function of the total iron content.^{17,30} The radiation-induced reduction and precipitation do not affect the associated Fe^{2+} ions. This is in agreement with other results on thermochemical reduction and oxidation of Fe in MgO, where despite extreme conditions, a certain proportion of the Fe^{2+} remains unaffected.^{13,31} The indi-

cation of Fe^{2+} as the likely diffusing entity is in agreement with theoretical calculations for the diffusion of Fe in MgO.³²

V. CONCLUSIONS

We may conclude that we are dealing with a radiation-induced reduction and precipitation process in which displacement damage and radiation enhanced diffusion play an important role. It would appear that, in contrast with the isolated Fe^{2+} ions which diffuse and aggregate with remarkable ease, diffusion of the impurity paired Fe^{2+} is inhibited.

The importance of radiation-enhanced diffusion in fusion materials need hardly be stressed. In any future fusion reactor environment, such a process could rapidly change quite markedly the properties of any refractory oxides employed.

ACKNOWLEDGMENTS

We are indebted to Mr. A. Mojado and Mr. E. Sánchez-Cabezudo for their continuous help with these experiments, and to Dr. R. Gonzalez and Dr. C. Ballesteros for the electron microscope measurements. We also thank Dr. Y. Chen for kindly supplying the Fe- and Ni-doped samples.

¹R. W. Davidge, *J. Mater. Sci.* **2**, 339 (1967).

²P. Hing and G. W. Groves, *J. Mater. Sci.* **7**, 422 (1972).

³A. Perez, G. Marest, B. D. Sawicka, J. A. Sawicki, and T. Tyliczszak, *Phys. Rev. B* **28**, 1227 (1983).

⁴M. M. Abraham, L. A. Boatner, W. H. Christie, F. A. Modine, T. Negas, R. M. Bunch, and W. P. Unruh, *J. Solid State Chem.* **51**, 1 (1985).

⁵Y. Chen, M. M. Abraham, and H. T. Tohver, *Phys. Rev. Lett.* **37**, 1757 (1976).

⁶B. Henderson and J. E. Wertz, *Adv. Phys.* **17**, 749 (1968).

⁷M. Srinivasan and T. G. Stoebe, *J. Appl. Phys.* **41**, 3726 (1970).

⁸C. N. Ahlquist, *J. Appl. Phys.* **46**, 14 (1975).

⁹K. L. Tsang and Y. Chen, *J. Appl. Phys.* **54**, 4531 (1983).

¹⁰R. L. Hansler and W. G. Segelken, *J. Phys. Chem. Solids* **13**, 124 (1960).

¹¹M. G. Abramishvili, V. I. Altukhov, T. L. Kalabegishvili, and V. G. Kvachadze, *Phys. Status Solidi B* **104**, 49 (1981).

¹²S. Clement and E. R. Hodgson, *Phys. Rev. B* **30**, 4684 (1984).

¹³F. A. Modine, E. Sonder and R. A. Weeks, *J. Appl. Phys.* **48**, 3514 (1977).

¹⁴G. W. Groves and M. E. Fine, *J. Appl. Phys.* **35**, 3587 (1964).

¹⁵M. M. Abraham, C. T. Butler, and Y. Chen, *J. Chem. Phys.* **55**, 3752 (1971).

¹⁶W. A. Sibley, J. L. Kolopus, and W. C. Mallard, *Phys. Status Solidi* **31**, 223 (1969).

¹⁷S. Clement and E. R. Hodgson, *Radiat. Eff.* **97**, 215 (1986).

¹⁸K. W. Blazey, *J. Phys. Chem. Solids* **38**, 671 (1977).

¹⁹E. Sonder, T. G. Stratton, and R. A. Weeks, *J. Chem. Phys.* **70**, 4603 (1979).

²⁰J. Narayan, Y. Chen, R. M. Moon, and R. W. Carpenter, *Philos. Mag. A* **49**, 287 (1984).

²¹J. Narayan and Y. Chen, *Philos. Mag. A* **49**, 475 (1984).

²²R. M. Bunch, W. P. Unruh, and M. V. Iverson, *J. Appl. Phys.* **58**, 1474 (1985).

²³O. S. Oen, Oak Ridge National Laboratory Report No. 3813, 1965 (unpublished).

²⁴W. A. Sibley and Y. Chen, *Phys. Rev.* **160**, 712 (1967).

²⁵G. P. Pells, Atomic Energy Research Establishment Report No. 10083, 1981 (unpublished).

²⁶R. A. Youngman, L. W. Hobbs, and T. E. Mitchell, *J. Phys. (Paris) Colloq.* **41**, C6-227 (1980).

²⁷D. R. Sempolinski and W. D. Kingery, *J. Am. Ceram. Soc.* **63**, 664 (1980).

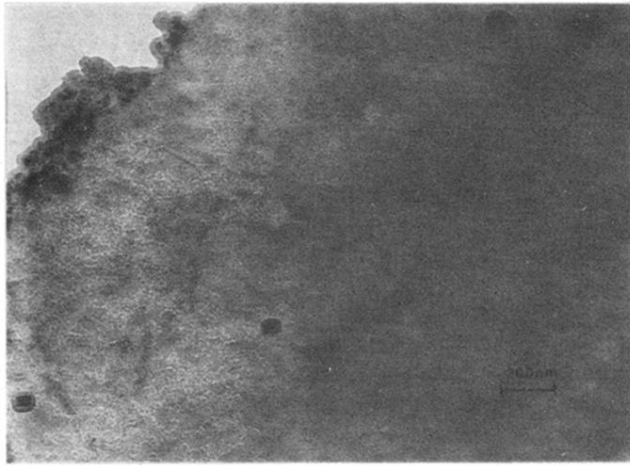
²⁸S. L. Blank and J. A. Pask, *J. Am. Ceram. Soc.* **52**, 669 (1969).

²⁹E. R. Hodgson, A. Delgado, and J. L. Alvarez Rivas, *J. Phys. C* **12**, 1239 (1979).

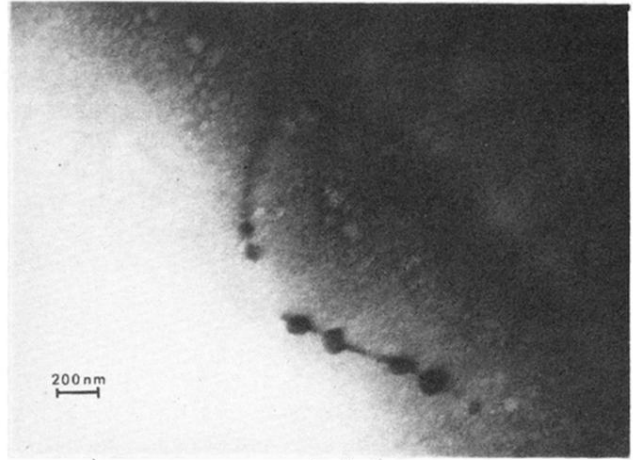
³⁰Y. Chen and W. A. Sibley, *Phys. Rev.* **154**, 842 (1967).

³¹R. A. Weeks, J. Gastineau, and E. Sonder, *Phys. Status Solidi A* **61**, 265 (1980).

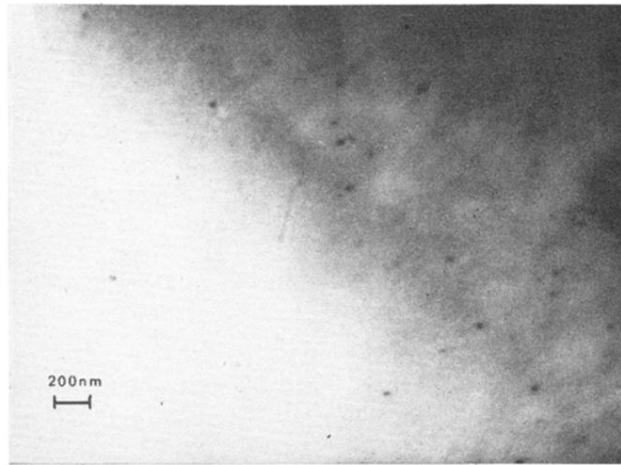
³²M. J. L. Sangster and A. M. Stoneham, *J. Phys. C* **17**, 6093 (1984).



(a)



(b)



(c)

FIG. 7. Electron micrographs showing iron-containing precipitates in the pure (a) and iron-doped samples (b) and (c) following irradiation at 650°C , $120 \mu\text{A cm}^{-2}$.